

## Direct observation of soliton dynamics in charge-density waves on a quasi-one-dimensional metallic surface

Harumo Morikawa, Iwao Matsuda, and Shuji Hasegawa

*Department of Physics, School of Science, University of Tokyo, 7-3-1 Hongo, Bunkyo-ku, Tokyo 113-0033, Japan*

(Received 24 February 2004; published 25 August 2004)

A periodic array of metallic In atomic chains on a Si(111) surface,  $4 \times 1$ -In superstructure, has been investigated by scanning tunneling microscopy at 6 K. We have found a lack of one-to-one correspondence between the filled- and empty-state images, meaning that the charge distribution is pinned on the frozen lattice in two ways. This supports the charge-density-wave (CDW) model rather than an order-disorder model, or a structural transition model, for the  $4 \times 1$  (room temperature) to  $8 \times 2'$  (low temperature) phase transition occurring on this surface. Furthermore, dynamics of a soliton in the CDW has been observed, which is characteristic of this kind of quasi-one-dimensional system.

DOI: 10.1103/PhysRevB.70.085412

PACS number(s): 68.35.Rh, 71.45.Lr

Low-dimensional electronic systems have attracted a great interest because of their exotic property such as Peierls transition and Tomonaga-Luttinger-liquid behaviors.<sup>1,2</sup> Among them, a considerable number of studies have been performed, especially for charge-density waves (CDWs), focusing on its dynamical behavior. The synthesis technology of bulky low-dimensional materials has enabled a great advance in this field.<sup>3</sup> Compared with such bulk materials, solid surfaces have a large advantage in directly observing such dynamics by atomic-resolution local probe methods, such as scanning tunneling microscopy/spectroscopy (STM/S). However, until recently, few candidates for CDWs in surface systems have been reported, in spite of their intrinsic low dimensionality;<sup>4-7</sup> the CDW transition may be, in many cases, prohibited by a significant influence from the substrate. One such candidate, however, is the chain-like superstructure, such as that formed by one monolayer (ML) of indium adsorbed on a Si(111) surface. The Si(111)  $4 \times 1$ -In surface phase is known from photoemission spectroscopy to show a quasi-one-dimensional (quasi-1D) metallic feature at room temperature (RT),<sup>8,9</sup> and to undergo a phase transition into an  $8 \times 2'$  phase at low temperature (LT) below  $\sim 120$  K.<sup>7,10</sup> The previous angle-resolved photoemission spectroscopy (ARPES) and STM studies showed good Fermi surface nesting at RT, an energy-gap opening, and the periodicity doubling along the metallic In chains accompanied by a periodic lattice distortion at LT.<sup>7,11</sup> These facts have led to a Peierls-type scenario and a CDW picture for the transition. However, an x-ray diffraction (XRD) study<sup>12</sup> and a first-principles calculation<sup>13</sup> were against the scenario, because large atomic displacements from the RT structure<sup>14</sup> were found at LT, much larger than those expected by a weak-coupling CDW picture, thus favoring a picture of an order-disorder type or a structural phase transition. On the other hand, recent studies of Raman spectroscopy<sup>15</sup> and dynamical low-energy electron diffraction,<sup>16</sup> again, supported the CDW picture by claiming that the atomic displacements were much smaller than those estimated by the XRD<sup>12</sup> and the calculation.<sup>13</sup> Furthermore, electrical conductivity measurements with a variable-temperature microscopic four-point probe method showed a clear metal-to-insulator transi-

tion through the transition temperature,<sup>10,17</sup> indicating an electronic transition rather than an order-disorder type.

Thus, although the nature of the periodicity doubling along the In chains at LT is still under controversy, the  $8 \times 2'$  LT phase has been attractive as a prototypical quasi-1D surface system.

In the present study, we have investigated this surface carefully by STM at 6 K, a much lower temperature than in the previous studies.<sup>7,18</sup> First, we obtain another convincing evidence supporting the CDW picture for the phase transition; the charge-density distribution with respect to the lattice was different from chain to chain. The charge distribution is pinned on the frozen lattice in two different ways at 6 K, so that the empty-state images, which mainly show the atomic structure, and the filled-state images, which mainly show the charge distribution, do not have a one-to-one correspondence between them. Second, we observe a soliton in the CDW moving around with high mobility even at a significantly low temperature of 6 K, which has been predicted by a theory for a similar quasi-1D system, such as polyacetylene.<sup>20,21</sup> This is a direct observation of such a soliton dynamics in real space with atomic resolution.

The experiment was carried out using a commercial ultrahigh-vacuum LT STM system (UNISOKU USM501-type). To make a single-domain (SD)  $4 \times 1$ -In surface superstructure, we used a vicinal Si(111) wafer (*P*-doped, *n*-type 11–100  $\Omega$  cm at RT) whose normal was  $1.8^\circ$  off from (111) toward  $[11\bar{2}]$  direction. The sample was cleaned in a standard way; flash heating by direct current up to 1500 K for a few seconds after mild degassing at 750 K for more than 12 h. We checked the clean  $7 \times 7$  structure by reflection high-energy electron diffraction (RHEED) and STM. Indium was evaporated from a well out-gassed alumina-coated tungsten basket. The SD Si(111)  $4 \times 1$ -In structure was prepared by 1 ML deposition of In onto the sample, which was kept at 800 K. The superstructure was checked by *in situ* RHEED observation. The sample was transferred into a cold stage at which STM measurements were carried out at 6 K. The temperature was measured by a thermocouple attached on the sample stage. All the STM images shown here were taken in constant-current mode. During our experiment, the pressure was kept at less than  $1 \times 10^{-10}$  Torr.

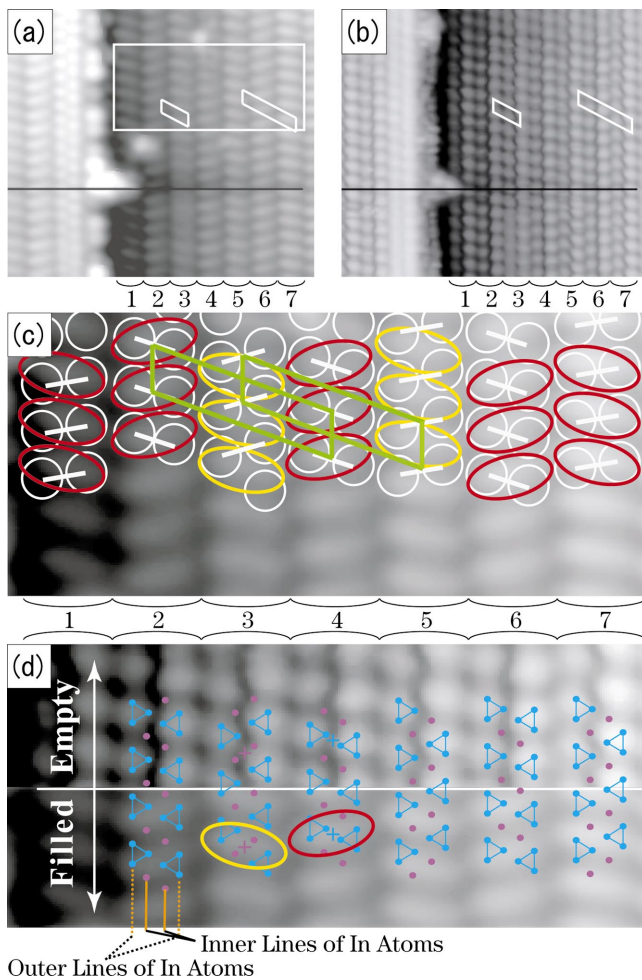


FIG. 1. (Color) (a) Filled- and (b) empty-state STM images of the same area ( $130 \times 150 \text{ \AA}$ ). The tip biases are 2.0 and  $-1.5 \text{ V}$ , respectively. The horizontal black line is the marker used to identify the same place. The  $4 \times 2$  and  $8 \times 2$  unit cells are drawn in (a) and (b) by white parallelograms. (c) An enlarged image of the rectangular area in (a). The white circles indicate the protrusions in the empty-state image (b). Red and yellow ellipses outline the cocoons in (a). The  $8 \times 2$  unit cells are drawn by green parallelograms. (d) The same area as (c), superimposed by a structure model proposed in Ref. 12. The upper half is the empty-state and the lower half is the filled-state images.

Figure 1 shows filled- and empty-state STM images of the same area on the sample surface. In the filled-state image (a), vertical chains of cocoon-like structures with the  $\times 2$  periodicity along the chains are observed, which is the same as in the previous STM study at 70 K,<sup>7</sup> but different from a theoretical simulation.<sup>13</sup> In the empty-state image (b), each chain splits into two rows; each cocoon changes into a pair of circular protrusions. The numbers from 1 to 7 at the bottom of the images identify the corresponding chains in the filled- and empty-state images. Hereafter, to avoid confusion, we use the word “chains” only for the stripes in the filled-state image with the chain numbers. We also use “subchains” for each line of protrusions in the empty state. One chain in the filled-state image consists of two subchains in the empty-state image. The  $4 \times 2$  and  $8 \times 2$  unit cells are drawn in (a) and (b) by white parallelograms.

Detailed correspondence between the filled and empty states is obtained by superimposing the two images with each other. White circles and colored ellipses in Fig. 1(c) trace protrusions in the empty-state image and the cocoons in the filled-state image at the identical area, respectively. In the filled-state image, each cocoon is tilted from the chain direction, rightside-up or leftside-up. The tilting direction is the same for all cocoons in each chain, while opposite between the adjacent chains. This ordering in the cocoon tilting across the chains produces  $\times 8$  periodicity in the  $8 \times 2'$ -In phase.

In the empty-state image, two subchains are slightly shifted with each other along the chain direction in each chain, so that pairs of white circles are tilted as indicated by tilted bars in (c). However, the tilting of the circle pairs is always opposite to the corresponding cocoon's tilting. If the cocoons are rightside-up, the circle pairs are leftside-up in the same chain.

An important feature is found here by comparing Chain Nos. 1, 2, 4, 6, and 7 [red cocoons in (c)] and Nos. 3, and 5 [yellow cocoons in (c)]. In the red-cocoon chains, each bar connecting the pair of white circles is located on each cocoon, while in the yellow-cocoon chains, the bars are located between the neighboring cocoons. In other words, the relation between the filled- and empty-state images is different between the red and yellow chains. As indicated by two  $8 \times 2$  unit cells drawn by green parallelograms, the pairs of circles in the yellow chains (Nos. 3 and 5) are shifted by  $a_0$  along the chain direction with respect to the red chains (Nos. 1, 2, 4, 6, and 7), where  $a_0$  is the length of the  $1 \times 1$  surface unit cell. But, for the cocoons in the filled-state image, such a shift between the red and yellow chains is not found. Thus we have found two types of correspondence between the ellipses and circles. In other words, *the correspondence between the filled- and the empty-state images is not one to one.*

To understand this phenomena more in detail, a structure model<sup>12,13</sup> is superimposed on the STM images in Fig. 1(d), where the upper half is the empty-state image, and the lower one, the filled state. Although the structure model of the  $8 \times 2'$  LT phase is under controversy,<sup>12,13,15,22</sup> there is a consensus that the double periodicity along the chains in the LT structure is formed by changing the atomic bond lengths along the chain; while the In-In spacings along the chain are regular in the  $4 \times 1$  phase at RT, they change to be longer and shorter alternately, making the  $\times 2$  periodicity along the chains at LT. Following the way of Kumpf *et al.*,<sup>12</sup> we express this model using indium-atom triangles that correspond to the circular protrusions in the empty-state image, as shown in Fig. 1(d). This correspondence between the model and the STM image is quite natural by considering the relation with the RT phase. A previous STM study<sup>23</sup> and a theoretical simulation<sup>13</sup> for the  $4 \times 1$  RT structure showed that the inner pair of indium lines are brighter in the filled-state, but darker in the empty-state, images. Our STM images at 6 K also show similar bias-polarity dependence in the middle of each chain. This indicates that the center line of a cocoon chain corresponds to the center of the inner lines of the four lines of indium atoms. In other words, the dark line between two adjacent cocoon chains in the filled-state image

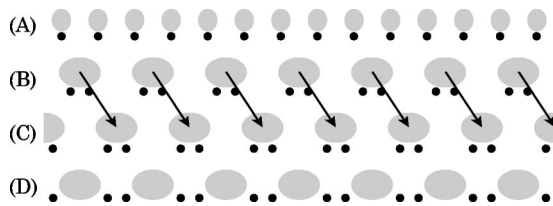


FIG. 2. Schematic illustrations of a normal 1D metallic chain (A), and its CDW states (B)–(D). The black circles and grey shadows represent atoms and electron clouds, respectively. (B) and (C) are in antiphase with each other. The domain boundary between (B) and (C) is a soliton, and the domain (B) changes to (C) as a soliton moves. (D) shows another way to pin the electron clouds on the same lattice as in (B) [and (C)], which is seen in yellow and red chains in Fig. 1 (see the text).

corresponds to Si zigzag chains between the four In lines.

Both the model and the STM image have a glide plane, which is consistent with diffraction results.<sup>12,16</sup> The correspondence between the model and STM images shown in Fig. 1(d), and another one in which the model is shifted by  $a_0$  along the chain direction with respect to the STM images (in which the circular protrusions in the empty-state image are located between the In-atom triangles), are the only ways to meet this symmetry requirement. Although we take here the way shown in Fig. 1(d), the other choice also works for the following discussion.

Now the unusual relation between the empty- and filled-state images in Fig. 1(c) is clear in 1(d). In Chain Nos. 3, and 5, lone indium atoms (purple dots) in the inner two lines of In atoms, which are free from the In-atom triangles (blue dots), are on the cocoons in the filled-state image, but they are located between the cocoons in Chain Nos. 1, 2, 4, 6, and 7. In other words, the cocoons do not necessarily correspond to the atomic arrangement. In the empty states, on the other hand, the lone indium atoms are always located between the circular protrusions. These features cannot be explained by a usual sense that the atomic structure uniquely corresponds to the distribution of protrusions in STM images (charge distribution). This unusual feature is, however, explained in the following way by assuming a CDW picture for this surface.

As indicated by crosses in Fig. 1(d), the center of a cocoon in the filled-state image is located at the middle of two neighboring lone indium atoms in the Chain Nos. 3, and 5, while at the middle of two neighboring indium triangles in Chain Nos. 1, 2, 4, 6, and 7. The charge has the maximum density at these inequivalent positions, but this is natural for CDW systems. When a CDW is commensurate with the lattice periodicity as in the present case, there is a strong locking effect between the CDW and the lattice potential. Two sites labeled by blue and purple crosses in Fig. 1(d) are symmetric points, corresponding to the local potential minima or maxima, and, thus, they are the possible locking sites. It is for this reason that the maxima of the charge density sit on these two points, indicating the existence of the two inequivalent locking sites in the superstructure. The situation is schematically shown in Fig. 2 as the difference between (B) and (D).

In this way, the unusual correspondence between the filled- and empty-state images is naturally understood in

terms of a commensurate CDW picture. The CDW system is simply expected to exhibit a contrast inversion between the filled- and empty-state STM images, because of the charge-density modulation leaving the charge-excess and charge-deficit regions. The center of cocoons in the filled-state image becomes dark in the empty state, indicating the charge redistribution in the inner two lines of In atoms, which is, roughly speaking, the expected one for the CDW in this sense. The previous first-principle calculation<sup>13</sup> for the RT structure showed that the two bands named  $m_2$  and  $m_3$ , which are responsible for the Fermi surface nesting, originate mainly from the inner two rows of In lines. It is because of this reason that the largest charge modulation is observed on the inner lines in each chain. But such a simple contrast inversion is not observed in other points in the unit cell, probably because the empty-state image mainly shows the atomic structure, while the filled-state one is strongly modulated by the charge distribution.

In the previous XRD study, a structural phase transition, rather than the CDW transition, was suggested based on the lack of complete long-range ordering of the ‘ $\times 8$ ’ periodicity across the chains even at 20 K.<sup>12</sup> A simple CDW picture may postulate a bichain periodicity across the chains, because the charge maxima in the neighboring CDW chains should avoid each other, leaving the neighboring CDW chains in antiphase (phase locking), as depicted by (B) and (C) in Fig. 2. Our STM image did not show the complete long-range order of such a bichain modulation even at 6 K, either. This is evident at the lowest part of Fig. 1(a), where the alternate tilting of cocoons in the chains is not uniform across the chains. However, by considering that the commensurability order of this CDW is  $M=2$ , a strong locking effect between the CDW and the lattice is expected. The locking effect is stronger between the CDW and the lattice, than between the neighboring CDW chains. The incomplete  $\times 8$  periodicity can be attributed to the two ways of CDW-lattice locking mentioned before [as depicted at (C) and (D) in Fig. 2].

Next, the dynamical changes in the CDW at this LT phase are shown. Figures 3(a)–3(e) are a series of STM images successively taken from the same area. A protrusion of the step labeled ‘‘A’’ is a marker to identify the position. The black arrows in (a)–(c) indicate a misty area in Chain No. 3, where the  $\times 2$  modulation along the chain is not so clear. The misty area is obvious on the left subchain of Chain No. 3 in (a) and (c), and the corresponding cocoons in the filled-state image is wholly obscure in (b). First, in the image (a), the misty area was located at the lower right of the marker ‘‘A.’’ The image (b) was taken 12 min later than (a) ( $t=12$  min), with opposite bias polarity. The misty area seems to shift slightly upwards along the chain. However, its motion is evident in (c), taken at  $t=18$  min: it shifts considerably downwards. And finally, in (d) and (e) taken at  $t=24$  and 30 min, respectively, there is no misty area in Chain No. 3 within the frame.

Figure 3(f) explains how the misty area causes shifts of the circular protrusions in the empty-state, and cocoons in the filled-state, images. The misty area is represented by a gray area in this illustration. Above the misty area, the right subchain of Chain No. 2 is higher than the left subchain of Chain No. 3 in the empty state, and the right cocoon edge of

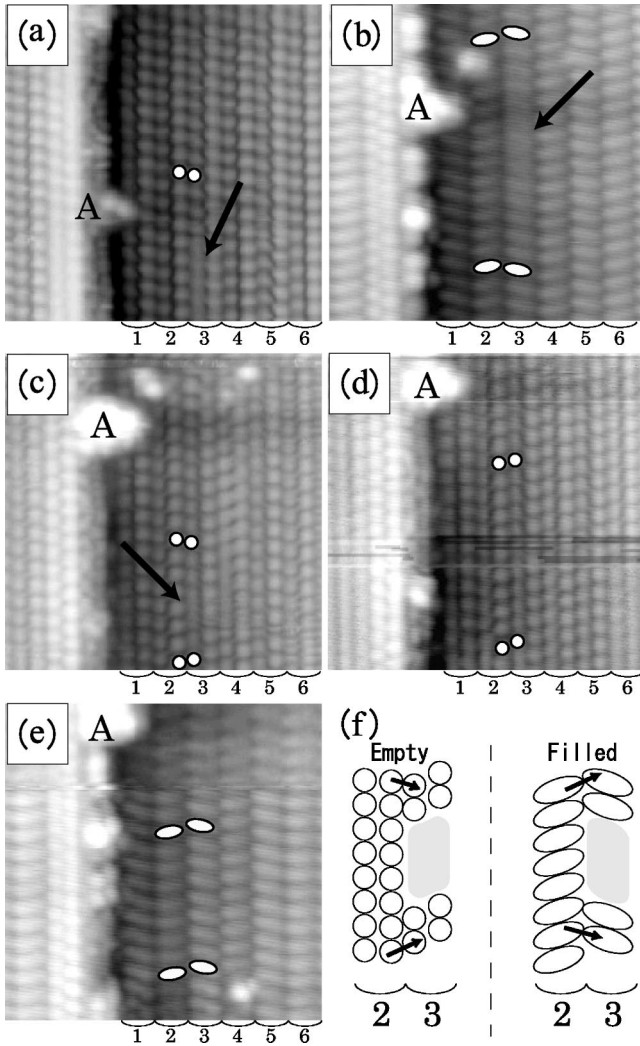


FIG. 3. (a)–(e) A series of STM images taken successively ( $130 \times 130 \text{ \AA}$ ). The elapsed time ( $t$ ) from the first imaging and the tip bias ( $V_T$ ) of each image are (a)  $t=0 \text{ min}$ ,  $V_T=-1.5 \text{ V}$ , (b)  $t=12 \text{ min}$ ,  $V_T=2.0 \text{ V}$ , (c)  $t=18 \text{ min}$ ,  $V_T=-1.5 \text{ V}$ , (d)  $t=24 \text{ min}$ ,  $V_T=-1.5 \text{ V}$ , and (e)  $t=30 \text{ min}$ ,  $V_T=2.0 \text{ V}$ . A protrusion marked as “A” indicates a marker for identifying the position. The black arrows in (a)–(c) indicate “uncertain phase areas” moving along chain (3). The relation between chains (2) and (3) is seen from white circles on (a), (c), and (d), and/or ellipses on (b) and (e), which leads to an illustration (f) showing the phase shift caused by the soliton in chain (3).

Chain No. 2 is lower than the left cocoon edge of Chain No. 3 in the filled state, as indicated by arrows in (f). But the situation is reversed below the misty area, as indicated by the arrows of opposite tilting. This relation between Chain Nos. 2 and 3 above and below the soliton can be seen from white ellipses and circles on the images (a)–(c). In (d), the relation of protrusions between Chain Nos. 2 and 3 is the same as that at the lower part of images (a) and (c), thus the misty area should have gone up from the frame. In contrast, in (e), the relation is the same as that of the upper part of the image (b). So the misty area should have come back after (d) and gone down from the frame before the image (e) is taken. Thus the misty area continues to move up and down along

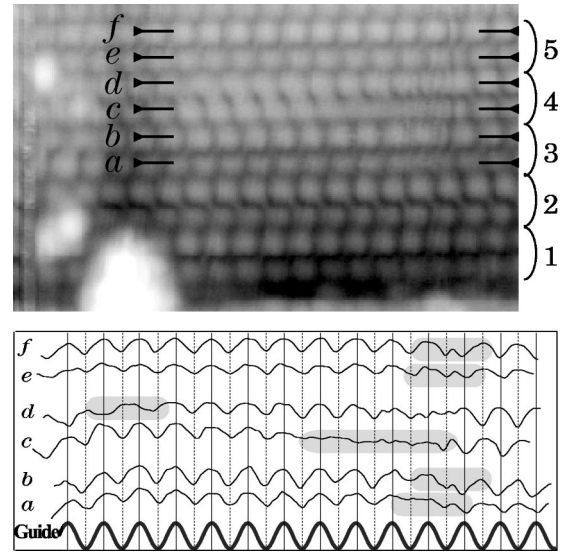


FIG. 4. A part of the STM image of Fig. 3(c), which is rotated by  $90^\circ$  (top panel), and the line profiles along the lines indicated in the STM image (lower panel). The gray shadow in the line profile indicates a misty area in each subchain.

the chain. Since our STM tip scans in the horizontal direction in the images from the top line to bottom one, the misty area cannot be dragged along the chains by the STM tip.<sup>19</sup> Thus, this dynamical behavior is not a tip effect, but a real nature of this surface.

We can also find this kind of dynamics in other chains. The role of the misty area upon the phase of the CDW modulation mentioned above is more clearly shown by line profile analysis. A part of the STM image [Fig. 3(c)] is shown in the upper panel of Fig. 4. The lower graph is the line profiles along six subchains labeled  $a$ – $f$  in the STM image. A sinusoidal curve at the bottom of the graph is just a guide of the phase. The profiles  $a$  and  $b$  are for subchains of Chain No. 3,  $c$  and  $d$  are for those in Chain No. 4, and  $e$  and  $f$  are for those in Chain No. 5. The misty area is indicated by gray shadows in the profiles. Both subchains  $a$  and  $b$  in Chain No. 3 undergo the phase shifts of  $\pi$  between the left- and right-hand sides of the misty area; the line profile on the left-hand side of the misty area is in phase with the guide sinusoidal curve, while on the right-hand side it is out of phase. Thus, the misty area acts as a phase shifter of the charge-density modulation. In Chain No. 5, two subchains,  $e$  and  $f$ , also have the same phase shifts simultaneously across the misty area as in Chain No. 3. However, in Chain No. 4, the phase shifts occur at different positions between the two subchains. In the left part, the profile  $c$  is out of phase with  $d$ , but in the middle area, both profiles are in phase, and in the right area, the phase is reversed from each other again. This restricts the structure model to one in which the two subchains can change their phase independently. The model used in Fig. 3(d) is acceptable from this point of view.

Now we shall characterize this dynamic phenomenon. Two types of phase modulation, named phason and soliton, are known for CDW systems. However, since the order of commensurability is  $M=2$  for the present CDW, the nesting vector  $\mathbf{Q}$  is half of the reciprocal lattice vector  $\mathbf{G}$ , i.e.,  $\mathbf{Q}$

$=\mathbf{G}/2$ . This leads to the following relations:  $b_{\mathbf{Q}}=b_{-\mathbf{Q}}, b_{\mathbf{Q}}^{\dagger}=b_{-\mathbf{Q}}^{\dagger}$ . Thus the CDW order parameter  $\Delta=g/\sqrt{2N_i}\langle b_{\mathbf{Q}}+b_{-\mathbf{Q}}^{\dagger}\rangle$  is real in this case, and the phason, which is related to the imaginary part of the order parameter, should be ruled out. Here we used  $b$  and  $b^{\dagger}$  as phonon annihilation and creation operators,  $N_i$  as the ion density, and  $g$  as the electron-phonon coupling constant. Thus this phenomenon should be a soliton, and the Su-Schrieffer-Heeger (SSH) theory<sup>20,21</sup> is applicable. From the previous ARPES results,<sup>7,8</sup> the CDW energy gap is  $\Delta=150$  meV and the Fermi wavenumber is  $k_F=0.4$  Å<sup>-1</sup>. Using these values, the length of a SSH soliton for the present system is estimated as  $2\xi_0=\hbar^2k_F/m_e\Delta\sim 40$  Å. On the other hand, the experimental length of a soliton should be measured using a stable one. In Fig. 3, some solitons were observed, but most of them were observed only in one image, meaning that their velocity was so fast compared with the STM scan. However, although it is not shown in the figure, just the same STM image as (b) was obtained at  $t=6$  min. Thus, one can consider that the misty area in Chain No. 3 stayed at nearly the same place during  $t=6-12$  min, and we can estimate from (b) the length to be  $\sim 50$  Å, which is consistent with the SSH theory.

Following discussion would be important to know the nature of the phase transition. Based on the SSH theory, a soliton is mobile because the lattice tends to be in the  $\times 1$  periodicity ordering, while the electron density tends to be in the  $\times 2$  ordering. That is, the balance between the energy cost, by lattice distortion, and the energy gain, by electronic redistribution, results in a highly mobile soliton (a domain boundary of two CDWs whose phases are reversed from each other). If the lattice would gain the energy by the  $\times 2$  restructuring, the domain boundary should not be mobile anymore. In this context, the present system is shown to be a pure CDW one, not a result or trigger of a structural reconstruction.<sup>12,13</sup>

It is also important to note that the unusual correspondence between the filled- and empty-state images shown in

Fig. 1 is *not* caused by the soliton motion. By comparing Figs. 3(a) and 3(b), one can see that the correspondence between filled- and empty states in each chain is the same as shown in Fig. 1, i.e., Chain Nos. 1 and 2 are red types and Chain No. 3 is a yellow one. One might assume that this phenomenon was caused by solitons that have passed along these chains *between*  $t=0$  and  $t=12$  min, that is, if two solitons have passed along Chain Nos. 1 and 2 between  $t=0$  and  $t=12$  min, the correspondence between filled- and empty-state images should be different between Chain Nos. 1–3. However, this assumption is ruled out by comparing (a) and (c). One can notice that the relation among subchains in Chain Nos. 1–3 is still the same in (c) ( $t=18$  min) and in (a) ( $t=0$ ). This means that no other soliton appeared in these chains other than the one observed in Chain No. 3 during the time. In other words, no solitons passed through between the imagings of (a) and (b) in Fig. 3. Thus, the unusual correspondence between the filled- and empty-state images cannot be explained by the motion of solitons.

The phase shift caused by a soliton is explained with schematic illustrations in Fig. 2. Since a soliton shifts the phase of CDW, both in filled and empty states as shown in Fig. 3, it is understood as a domain boundary of two CDWs [(B) and (C)], which are in antiphase with each other. On the other hand, the unusual correspondence between the opposite bias polarities mentioned in Fig. 1 results from the two ways of CDW-lattice locking [(C) and (D)].

In summary, a detailed STM observation at 6 K has been performed for a 1D chain structure of the Si(111)  $4\times 1$ -In surface. Based on the detailed analysis about the correspondence between the filled- and empty-state images, we have shown evidence of the CDW scenario for the  $4\times 1\rightarrow 8\times 2'$  phase transition. We also have shown the dynamics of SSH solitons, which are expected for a commensurate CDW.

This work has been supported by Grants-In-Aid from the Japanese Society for the Promotion of Science.

- <sup>1</sup>R. E. Peierls, *Quantum Theory of Solids* (Clarendon, Oxford, 1964).
- <sup>2</sup>J. M. Luttinger, *J. Math. Phys.* **4**, 1154 (1963).
- <sup>3</sup>G. Grüner, *Density Waves in Solids*, 1st ed. (Addison-Wesley, Reading, MA, 1994).
- <sup>4</sup>J. M. Carpinelli, H. H. Weitering, E. W. Plummer, and R. Stumpf, *Nature (London)* **381**, 398 (1996).
- <sup>5</sup>J. M. Carpinelli, H. H. Weitering, M. Bartkowiak, R. Stumpf, and E. W. Plummer, *Phys. Rev. Lett.* **79**, 2859 (1997).
- <sup>6</sup>T. Aruga, *J. Phys.: Condens. Matter* **14**, 8393 (2002).
- <sup>7</sup>H. W. Yeom, *et al.*, *Phys. Rev. Lett.* **82**, 4898 (1999).
- <sup>8</sup>T. Abukawa, M. Sasaki, F. Hisamatsu, T. Goto, T. Kinoshita, A. Kakizaki, and S. Kono, *Surf. Sci.* **325**, 33 (1995).
- <sup>9</sup>T. Kanagawa, R. Hobara, I. Matsuda, T. Tanikawa, A. Natori, and S. Hasegawa, *Phys. Rev. Lett.* **91**, 036805 (2003).
- <sup>10</sup>T. Tanikawa, T. Kanagawa, R. Hobara, I. Matsuda, and S. Hasegawa, *Phys. Rev. Lett.* **93**, 016801 (2004).
- <sup>11</sup>O. Gallus, T. Pillo, M. Hengsberger, P. Segovia, and Y. Baer, *Eur.*

- Phys. J. B* **20**, 313 (2001).
- <sup>12</sup>C. Kumpf, O. Bunk, J. H. Zeysing, Y. Su, M. Nielsen, R. L. Johnson, R. Feidenhans'l, and K. Bechgaard, *Phys. Rev. Lett.* **85**, 4916 (2000).
- <sup>13</sup>J.-H. Cho, D.-H. Oh, K. S. Kim, and L. Kleinman, *Phys. Rev. B* **64**, 235302 (2001).
- <sup>14</sup>O. Bunk, G. Falkenberg, J. H. Zeysing, L. Lottermoser, R. L. Johnson, M. Nielsen, F. Berg-Rasmussen, J. Baker, and R. Feidenhans'l, *Phys. Rev. B* **59**, 12 228 (1999).
- <sup>15</sup>K. Fleischer, S. Chandola, N. Esser, W. Richter, and J. F. McGilp, *Phys. Rev. B* **67**, 235318 (2003).
- <sup>16</sup>S. Mizuno, Y. O. Mizuno, and H. Tochiyama, *Phys. Rev. B* **67**, 195410 (2003).
- <sup>17</sup>T. Tanikawa, I. Matsuda, R. Hobara, and S. Hasegawa, *e-J. Surf. Sci. Nanotech.* **1**, 50 (2003).
- <sup>18</sup>S. V. Ryjkov, T. Nagao, V. G. Lifshits, and S. Hasegawa, *Surf. Sci.* **488**, 15 (2001).

- <sup>19</sup>The shorter length of the misty area in Fig. 3(c) than in 3(a) and 3(b) implies that it is moving upward during the scan.
- <sup>20</sup>W.-P. Su, J. R. Schrieffer, and A. J. Heeger, Phys. Rev. Lett. **42**, 1698 (1979).
- <sup>21</sup>W.-P. Su, J. R. Schrieffer, and A. J. Heeger, Phys. Rev. B **22**, 2099 (1980).
- <sup>22</sup>H. W. Yeom, K. Horikoshi, H. M. Zhang, K. Ono, and R. I. G. Uhrberg, Phys. Rev. B **65**, 241307 (2002).
- <sup>23</sup>A. A. Saranin, A. V. Zotov, K. V. Ignatovich, V. G. Lifshits, T. Numata, O. Kubo, H. Tani, M. Katayama, and K. Oura, Phys. Rev. B **56**, 1017 (1997).